Gene expression signatures for identifying diffuse-type gastric cancer associated with epithelial-mesenchymal transition

SHIHORI TANABE[1], KAZUHIKO AOYAGI[2], HIROSHI YOKOZAKI[3] and HIROKI SASAKI[2]

[1]Division of Safety Information on Drug, Food and Chemicals, National Institute of Health Sciences, 1-18-1, Kami-yoga, Setagaya-ku, Tokyo 158-8501; [2]Department of Translational Oncology, National Cancer Center Research Institute, 1-1, Tsukiji 5-chome, Chuo-ku, Tokyo 104-0045; [3]Department of Pathology, Kobe University Graduate School of Medicine, 7-5-1, Kusunoki-cho, Chuo-ku, Kobe 650-0017, Japan

Received February 7, 2014; Accepted March 28, 2014

DOI: 10.3892/ijo.2014.2387

Abstract. Epithelial-mesenchymal transition (EMT) is associated with tumor malignancy. The hedgehog-EMT pathway is preferentially activated in diffuse-type gastric cancer (GC) compared with intestinal-type GC; however, histological typing is currently the only method for distinguishing these two major types of GC. We compared the gene expression profiles of 12 bone marrow-derived mesenchymal stem cell cultures and 5 diffuse-type GC tissue samples. Numerous upregulated or downregulated genes were identified in diffuse-type GC, including *CDH1*, *CDH2*, *VIM*, *WNT4* and *WNT5*. Among these genes, the mRNA ratio of *CDH2* to *CDH1* could distinguish the 15 diffuse-type GC samples from the 17 intestinal-type GC samples. Our results suggested that the mesenchymal features were more prominent in diffuse-type GC than in intestinal-type GC, but were weaker in diffuse-type GC than in mesenchymal stem cells. Diffuse-type GC that has undergone extensive EMT, which has a poor prognosis, can be identified by quantitative PCR analysis of only two genes.

Introduction

Gene expression is dramatically deregulated in tumor development and progression. Various epithelial cell-derived cancers often have mesenchymal features. Epithelial-mesenchymal transition (EMT) is a physiological phenotypic shift in which epithelial cells with cell-cell and cell-extracellular matrix connections transform into mesenchymal cells and then migrate to other locations within the body (1). EMT is a key developmental process that is often activated during cancer invasion and metastasis, and EMT in immortalized human mammary epithelial cells results in the development of mesenchymal cells and the expression of stem-cell markers (2). These insights highlight the need to investigate the relationship between cancer and mesenchymal cells. Cancer genomic landscapes have been revealed, and mutations in cancer-associated genes involved in cell proliferation have been discovered (3). Here, we report that the expression of several genes involved in EMT or stem cell development is altered in cancer cells and mesenchymal stem cells (MSCs).

Gastric cancer (GC) is one of the leading causes of cancer-related deaths worldwide. Histopathologically, GC can be divided into two major categories: intestinal-type and diffuse-type. Intestinal-type GC develops via sequential stages including *Helicobacter pylori* (*H. pylori*)-associated gastritis, intestinal metaplasia (IM) and dysplasia. This type is found predominantly in high-risk geographic areas, such as East Asia, and is strongly correlated with the prevalence of *H. pylori* infection among the elderly. In contrast, diffuse-type GC appears in half of all GC cases and is more geographically dispersed. Diffuse-type GC typically develops from *H. pylori*-free, morphologically normal gastric mucosa without atrophic gastritis, or IM, and is both genetically and phenotypically different from intestinal-type GC (4-8). Unlike the decreasing incidence of intestinal-type GC, the prevalence of diffuse-type GC is reportedly increasing worldwide. Therefore, the molecular characterization of diffuse-type GC, with a particular focus on its infiltrating and scattered growth, is important for the development of novel therapeutics for this disease. The infiltrating and scattered growth of diffuse-type GC has been reported to be mediated by the loss of E-cadherin [cadherin 1, type 1, E-cadherin (epithelial) (*CDH1*)] function through somatic mutation, promoter methylation and cancer-associated downregulation (9). We previously reported that the activation of hedgehog (Hh) signaling selectively occurs in diffuse-type GC and that blocking the Hh signal inhibits the growth of GC cells in which Hh has been activated (6). We also reported that the EMT regulator ZEB1/SIP1 is a target of Hh signaling in diffuse-type GC and that ZEB1 regulates mesenchymal-related genes *WNT5A*, *CDH2* [*cadherin 2, type 1, N-cadherin (neuronal)*], *PDGFRB*, *EDNRA*, *ROBO1*, *ROR2* (*receptor tyrosine kinase-like orphan receptor 2*) and

Correspondence to: Dr Shihori Tanabe, Division of Safety Information on Drug, Food and Chemicals, National Institute of Health Sciences, 1-18-1, Kami-yoga, Setagaya-ku, Tokyo 158-8501, Japan
E-mail: stanabe@nihs.go.jp

Key words: epithelial-mesenchymal transition, microarray, mesenchymal stem cell, gastric cancer, gene expression

MEF2C that are preferentially expressed in diffuse-type GC (7). Thus, the hedgehog-EMT pathway is preferentially activated in diffuse-type GC compared with intestinal-type GC; however, histological typing is currently the only method to distinguish the two major types. Here, we report that diffuse-type GC that has undergone extensive EMT, which has a poor prognosis, was distinguished from intestinal-type GC by quantitative real-time RT-PCR analysis of only two genes.

Materials and methods

Cell culture. Human MSCs from bone marrow (Lonza, Walkersville, MD, USA) were cultured in mesenchymal stem cell growth medium (MSCGM; Lonza #PT-3001; MSC basal medium supplemented with mesenchymal cell growth supplement, L-glutamine, and penicillin/streptomycin) at 37˚C in a 5% CO_2 incubator. The cells were passaged according to the manufacturer's protocol, with a slight modification in the use of trypsin-EDTA solution (Lonza #CC-3232). The following lot numbers of human MSC batches were utilized: #4F1127, #4F0312, #5F0138, #4F1560, #4F0591 and #4F0760. Informed consent was obtained for the development of the Poietics human mesenchymal stem cell systems (Lonza) (10).

Total RNA purification and extraction. The MSCs were cultured on a 10-cm dish, lysed in 600 μl of buffer RLT (RNeasy lysis buffer) with β-mercaptoethanol, and homogenized using a QIA shredder (Qiagen, Düsseldorf, Germany). Total RNA was purified using RNeasy mini spin columns according to the manufacturer's protocol (Qiagen). Total RNA was eluted with RNase-free water (10). Cancer samples were lysed with Isogen lysis buffer and total RNA was extracted by precipitation with isopropanol (11).

Microarray analysis. Total RNA (100 ng) was reverse transcribed and amplified using a GeneChip kit (Affymetrix, Santa Clara, CA, USA). The microarray analysis was performed using GeneChip Human Genome U95Av2 or U133 Plus2.0 (Affymetrix) in accordance with the manufacturer's instructions (10,11). Human bone marrow-derived MSCs are commercially available from Lonza, and gastric cancer cells were obtained from the National Cancer Center Research Institute. The microarray data on human MSCs and gastric cancer are available to the public in NCBI's Gene Expression Omnibus (GEO) database and are accessible via GEO Series accession number GSE7888 and GSE42252, respectively (10,12).

Quantitative real-time RT-PCR analysis. Real-time RT-PCR was performed using primer sets designed for detecting *CDH1* (5'-GGGGTAGTGAGGATCTTGAT-3' and 5'-TCCTTTTCC ACCCCCAAAGA-3'), *CDH2* (5'-GGCATAGTCTATGGA GAAGT-3' and 5'-GCTGTTGTCAGAAGTCTCTC-3') and *VIM* (5'-GCTTTCAAGTGCCTTTCTGC-3' and 5'-GTT GGTTGGATACTTGCTGG-3'). Quantitative real-time PCR was performed using a Bio-Rad iCycler with iQ SYBR-Green Super mix as previously reported (11). The relative mRNA expression level of each gene was normalized to that of *ACTB* (β-actin: 5'-GAAGTCCCTTGCCATCCTAA-3' and 5'-GCA CGAAGGCTCATCATTCA-3') using the ΔΔCt method.

Statistics. Student's t-test or Wilcoxon's U test was performed to calculate the P-values. Microsoft Excel and GeneSpring software (Agilent Technologies, Ltd., CA, USA) were used for the analyses.

Results

Comparing the expression of EMT-related genes in MSCs and diffuse-type GC. The microarray gene expression analysis identified 51 upregulated probe sets that had detectable cells in either all of the 12 MSC samples or all of the 5 diffuse-type GC samples; the average GAPDH-normalized signal intensity of these upregulated probe sets in MSCs was >10-fold higher than the average GAPDH-normalized signal intensity in diffuse-type GC ($P<0.0001$) (Tables I and II). This class of probe sets contained probes recognizing *CDH2*, which encodes N-cadherin, a protein that has been reported to be involved in EMT (13). *CDH2* was upregulated in 12 MSC samples compared with the 5 diffuse-type GC samples (Fig. 1A). A previous report demonstrated that *CDH2* is a marker of EMT (13). E-cadherin stabilizes cellular organization or conformation (14). The expression of *CDH1* (E-cadherin), which plays an important role in the cell junctions of epithelial cells, was downregulated in MSCs compared with diffuse-type GC (Fig. 1B). It has been reported that HMLER cancer cells (human mammary epithelial cells transformed with genomic versions of SV40 large-T, *hTERT* and H-*ras*V12) have an increased $CD44^{high}/CD24^{low}$ cancer stem cell (CSC) fraction after treatment with small interfering RNA targeting *CDH1* (15,16). This report details the involvement of CDH1 in interfering with the CSC phenotype and in inducing stem cell differentiation. Considering the expression patterns of *CDH2* and *CDH1* in MSCs and diffuse-type GC, most of the cells in diffuse-type GC are likely to have an epithelial-like phenotype, although there is more evidence of EMT in diffuse-type GC than in intestinal-type GC.

We further examined mesenchymal phenotype-related genes in 5 diffuse-type GC samples and identified 1461 upregulated probe sets with an average signal intensity >500 in the 12 MSC samples and with greater than a 2-fold change in the 12 MSC samples compared with the 5 diffuse-type GC samples using the U133Plus2.0 platform. Of these 1461 probe sets, 983 were aligned with the U95Av2 platform. Using the U95Av2 platform, 94 probe sets were determined to be upregulated in the 13 diffuse-type GC samples compared with the 17 intestinal-type GC samples (Fig. 2). Probe sets that recognized the same symbol were unified in probe sets with a larger fold-change and 77 genes were selected (Table III). *FN1* (*fibronectin 1*) was upregulated in MSCs compared with diffuse-type GC (Fig. 3A). It has been reported that salinomycin has selective toxicity in the stem cells of epithelial cell-derived cancers and that it induces epithelial cell differentiation (17). Salinomycin, a selective breast cancer stem cell inhibitor, has been reported to decrease stem cell-related genes such as *CCND1* (*cyclin D1*), *LEF1* and *FN1*, which are targets of Wnt signaling (17). The role of Wnt signaling in different cell types may be an interesting target for cancer stem cell machinery (18,19). Gene expression was analyzed to investigate whether these stem cell-related genes were involved in the cellular phenotypic changes. *FN1* was upregulated in MSCs compared with diffuse-type GC,

Table I. Upregulated probe sets in MSCs compared with diffuse-type GC.

Probe set ID	Gene symbol	Gene title	Ratio	P-value (non-equal variance)	P-value (equal variance)	Entrez gene ID
206157_at	PTX3	Pentraxin 3, long	56.9	1.303E-11	2.124E-11	5806
214702_at	FN1	Fibronectin 1	43.7	1.116E-10	6.76E-10	2335
215446_s_at	LOX	Lysyl oxidase	14.8	5.836E-10	6.504E-09	4015
207558_s_at	PITX2	Paired-like homeodomain 2	11.7	1.076E-09	5.864E-08	5308
202952_s_at	ADAM12	ADAM metallopeptidase domain 12	19.5	4.79E-09	3.948E-07	8038
214701_s_at	FN1	Fibronectin 1	26.6	3.694E-08	4.612E-07	2335
204421_s_at	FGF2	Fibroblast growth factor 2 (basic)	10.9	6.115E-08	1.72E-06	2247
233533_at	KRTAP1-5	Keratin associated protein 1-5	163.7	6.246E-08	7.787E-07	83895
209946_at	VEGFC	Vascular endothelial growth factor C	13.7	6.864E-08	1.278E-06	7424
203438_at	STC2	Atanniocalcin 2	50.2	6.959E-08	9.427E-07	8614
228367_at	ALPK2	α-kinase 2	21.4	7.576E-08	1.14E-06	115701
239367_at	BDNF	Brain-derived neurotrophic factor	16.5	1.442E-07	3.538E-06	627
203439_s_at	STC2	Stanniocalcin 2	54.7	3.842E-07	6.59E-06	8614
201387_s_at	UCHL1	Ubiquitin carboxyl-terminal esterase L1 (ubiquitin thiolesterase)	13.9	6.127E-07	1.232E-05	7345
207345_at	FST	Follistatin	11.6	7.941E-07	1.709E-05	10468
204948_s_at	FST	Follistatin	22.5	1.041E-06	2.488E-05	10468
204298_s_at	LOX	Lysyl oxidase	54.2	1.615E-06	3.207E-05	4015
203851_at	IGFBP6	Insulin-like growth factor binding protein 6	10.2	1.752E-06	5.669E-05	3489
226847_at	FST	Follistatin	23.0	1.913E-06	4.582E-05	10468
219789_at	NPR3	Natriuretic peptide receptor C/guanylate cyclase C (atrionatriuretic peptide receptor C)	58.1	2.108E-06	4.278E-05	4883
206307_s_at	FOXD1	Forkhead box D1	11.1	2.308E-06	0.0001004	2297
236532_at	C11orf87	Chromosome 11 open reading frame 87	181.3	3.351E-06	6.966E-05	399947
213791_at	PENK	Proenkephalin	18.6	3.43E-06	9.108E-05	5179
203440_at	CDH2	Cadherin 2, type 1, N-cadherin (neuronal)	19.8	6.446E-06	0.0001663	1000
219729_at	PRRX2	Paired related homeobox 2	16.9	6.459E-06	0.0001542	51450
243813_at	LINC00968	Long intergenic non-protein coding RNA 968	47.0	8.462E-06	0.0001846	100507632
210261_at	KCNK2	Potassium channel, subfamily K, member 2	11.0	1.158E-05	0.0003414	3776
206382_s_at	BDNF	Brain-derived neurotrophic factor	44.6	1.159E-05	0.0002555	627
1557181_s_at	C11orf87	Chromosome 11 open reading frame 87	293.2	1.54E-05	0.0003308	399947
219054_at	NPR3	Natriuretic peptide receptor C/guanylate cyclase C (atrionatriuretic peptide receptor C)	28.3	1.911E-05	0.0004216	4883
1557180_at	C11orf87	Chromosome 11 open reading frame 87	21.7	2.153E-05	0.0004803	399947
235417_at	SPOCD1	SPOC domain containing 1	30.2	2.557E-05	0.0005603	90853
223618_at	FMN2	Formin 2	22.2	2.976E-05	0.0006566	56776
209905_at	HOXA10-HOXA9, HOXA9, MIR196B	HOXA10-HOXA9 readthrough, homeobox A9, microRNA 196b	11.2	3.068E-05	0.0008075	100534589, 3205, 442920
210367_s_at	PTGES	Prostaglandin E synthase	19.0	3.112E-05	0.0006888	9536
201107_s_at	THBS1	Thrombospondin 1	27.7	3.53E-05	0.0007676	7057
213707_s_at	DLX5	Distal-less homeobox 5	11.7	4.045E-05	0.0009757	1749
239202_at	RAB3B	RAB3B, member RAS oncogene family	11.8	4.595E-05	0.0010932	5865

Table I. Continued.

Probe set ID	Gene symbol	Gene title	Ratio	P-value (non-equal variance)	P-value (equal variance)	Entrez gene ID
204602_at	DKK1	Dickkopf 1 homolog (*Xenopus laevis*)	11.7	4.785E-05	0.0013798	22943
210121_at	B3GALT2	UDP-Gal:βGlcNAc β 1,3-galactosyltransferase, polypeptide 2	12.4	4.992E-05	0.0011294	8707
232122_s_at	VEPH1	Ventricular zone expressed PH domai homolog 1 (zebrafish)	11.9	6.254E-05	0.0015563	79674
229641_at	CCBE1	Collagen and calcium binding EGF domains 1	18.2	6.7E-05	0.001394	147372
1555471_a_at	FMN2	Formin 2	13.8	6.858E-05	0.0016045	56776
219790_s_at	NPR3	Natriuretic peptide receptor C/guanylate cyclase C (atrionatriuretic peptide receptor C)	50.1	7.041E-05	0.0014166	4883
222862_s_at	AK5	Adenylate kinase 5	15.3	7.202E-05	0.0015601	26289
1552487_a_at	BNC1	Basonuclin 1	11.7	8.369E-05	0.0019519	646
230112_at	MARCH4	Membrane-associated ring finger (C3HC4) 4, E3 ubiquitin protein ligase	15.3	8.722E-05	0.0019912	57574
244623_at	KCNQ5	Potassium voltage-gated channel, KQT-like subfamily, member 5	11.3	9.102E-05	0.0018888	56479
213640_s_at	LOX	Lysyl oxidase	29.9	9.205E-05	0.0018414	4015
217452_s_at	B3GALT2	UDP-Gal:βGlcNAc β 1,3-galactosyltransferase, polypeptide 2	13.0	9.284E-05	0.0019809	8707
235548_at	APCDD1L	Adenomatosis polyposis coli downregulated 1-like	36.2	9.734E-05	0.0019595	164284

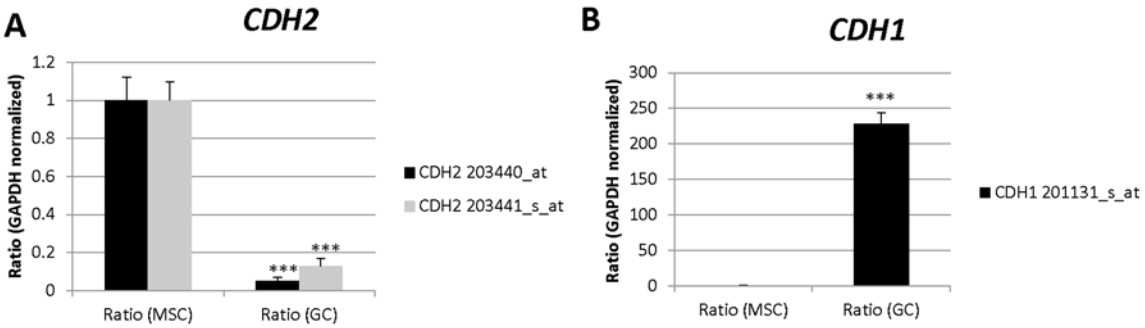

Figure 1. Gene expression of the two cadherins. (A) *CDH2* (N-cadherin) gene expression was upregulated in MSCs compared with diffuse-type GC. (B) *CDH1* (E-cadherin) gene expression was downregulated in MSCs compared with diffuse-type GC. The data are presented as the mean ± SE of the ratio to the average in the MSCs (***P<0.001 vs. MSCs; n=12 MSCs and n=5 diffuse-type GCs). The data were normalized to *GAPDH*.

suggesting that the stem cell phenotype was more typical in MSCs than in diffuse-type GC (Fig. 3A). One of the probe sets recognizing *VIM* (*vimentin*) was upregulated in diffuse-type GC compared with MSCs (Fig. 3B).

Comparing the expression of stem cell-related genes in MSCs and diffuse-type GC. To identify markers of EMT or the stemness phenotype of diffuse-type GC, we compared the expression of stem cell-related genes in MSCs and diffuse-type GC. We first selected stem-cell related genes based on biological processes using gene ontology and then performed a clustering analysis of the signal intensity of 33 stem cell-related genes that had greater than a 5-fold change in the *GAPDH*-normalized signal intensity in GC compared with MSCs (NCSS2007) (Fig. 4A). Among these 33 stem cell-related genes, 10 were selected that were significantly differentially expressed (more than a 20-fold change; P<0.01 and P<0.05; n=12 MSCs and n=5 diffuse-type GCs) (Fig. 4B). *SOX2*, which is involved in embryonic and adult tissue stem cell maintenance, was upregulated in diffuse-type GC compared with MSCs. This corresponded with previous reports indicating that *SOX2* was overexpressed or mutated in a stage-dependent

Table II. Gene ontology of upregulated genes in MSCs compared to diffuse-type GC.

Probe set ID	Gene symbol	Gene ontology biological process
202952_s_at	ADAM12	Proteolysis, cell adhesion, epidermal growth factor receptor signaling pathway, myoblast fusion
222862_s_at	AK5	Nucleobase-containing compound metabolic process, nucleoside diphosphate phosphorylation, ADP biosynthetic process, dADP biosynthetic process, signal transduction, nucleoside triphosphate biosynthetic process, pyrimidine ribonucleotide biosynthetic process, nucleobase-containing small molecule interconversion, phosphorylation, small molecule metabolic process, ATP metabolic process, nucleobase-containing small molecule metabolic process
228367_at	ALPK2	Protein phosphorylation, phosphorylation
235548_at	APCDD1L	-
210121_at 217452_s_at	B3GALT2	Protein glycosylation, oligosaccharide biosynthetic process
239367_at 206382_s_at	BDNF	Ureteric bud development, behavioral fear response, response to hypoxia, chronic inflammatory response, mitochondrial electron transport, NADH to ubiquinone, nervous system development, negative regulation of neuroblast proliferation, axon guidance, axon target recognition, behavior, learning or memory, feeding behavior, neuron recognition, response to hormone stimulus, glutamate secretion, response to fluoxetine, dendrite development, regulation of metabolic process, nerve development, response to nutrient levels, response to vitamin A, mechanoreceptor differentiation, response to drug, fear response, negative regulation of apoptotic process, regulation of neuron apoptotic process, negative regulation of neuron apoptotic process, positive regulation of neuron differentiation, negative regulation of striated muscle tissue development, regulation of retinal cell programmed cell death, regulation of synaptic plasticity, regulation of long-term neuronal synaptic plasticity, positive regulation of long-term neuronal synaptic plasticity, regulation of short-term neuronal synaptic plasticity, inner ear development, cognition, positive regulation of synapse assembly, response to hyperoxia, regulation of excitatory postsynaptic membrane potential, response to anesthetic
1552487_a_at	BNC1	Transcription, DNA-dependent, regulation of transcription, DNA-dependent, regulation of transcription from RNA polymerase I promoter, regulation of transcription from RNA polymerase II promoter, positive regulation of cell proliferation, epidermis development, wound healing, positive regulation of epithelial cell proliferation, chromosome organization
236532_at 1557180_at 1557181_s_at	C11orf87	-
229641_at	CCBE1	Angiogenesis, lymphangiogenesis, sprouting angiogenesis, multicellular organismal development, venous blood vessel morphogenesis
203440_at	CDH2	Cell adhesion, homophilic cell adhesion, heterophilic cell-cell adhesion, synapse assembly, cell-cell adhesion, calcium-dependent cell-cell adhesion, cell migration, regulation of myelination, regulation of protein localization, cell junction assembly, adherens junction organization, regulation of Rho protein signal transduction, muscle cell differentiation, positive regulation of MAPK cascade, cell-cell junction organization, blood vessel morphogenesis, regulation of axonogenesis, striated muscle cell differentiation, positive regulation of muscle cell differentiation, negative regulation of canonical Wnt receptor signaling pathway
204602_at	DKK1	Negative regulation of transcription from RNA polymerase II promoter, cell morphogenesis involved in differentiation, endoderm formation, mesoderm formation, hair follicle development, regulation of receptor internalization, multicellular organismal development, endoderm development, Wnt receptor signaling pathway, regulation of Wnt receptor signaling pathway, negative regulation of Wnt receptor signaling pathway, embryonic limb morphogenesis, negative regulation of BMP signaling pathway, forebrain development, negative regulation of protein complex assembly, response to retinoic acid, negative regulation of peptidyl-serine phosphorylation, negative regulation of mesodermal cell fate specification, regulation of endodermal cell fate specification, negative

Table II. Continued.

Probe set ID	Gene symbol	Gene ontology biological process
		regulation of skeletal muscle tissue development, head morphogenesis, face morphogenesis, negative regulation of pathway-restricted SMAD protein phosphorylation, positive regulation of heart induction by negative regulation of canonical Wnt receptor signaling pathway, negative regulation of canonical Wnt receptor signaling pathway, Wnt receptor signaling pathway involved in somitogenesis, extracellular negative regulation of signal transduction, negative regulation of canonical Wnt receptor signaling pathway involved in cardiac muscle cell fate commitment, negative regulation of cardiac muscle cell differentiation
213707_s_at	DLX5	Skeletal system development, ossification, osteoblast differentiation, endochondral ossification, transcription, DNA-dependent, regulation of transcription, DNA-dependent, multicellular organismal development, nervous system development, axonogenesis, axon guidance, cell proliferation, embryonic limb morphogenesis, BMP signaling pathway, epithelial cell differentiation, inner ear morphogenesis, ear development, positive regulation of osteoblast differentiation, positive regulation of transcription, DNA-dependent, positive regulation of transcription from RNA polymerase II promoter, anatomical structure formation involved in morphogenesis, positive regulation of epithelial cell proliferation, palate development, olfactory pit development, head development, face morphogenesis, bone morphogenesis, cellular response to BMP stimulus, positive regulation of canonical Wnt receptor signaling pathway, positive regulation of transcription from RNA polymerase II promoter involved in cellular response to chemical stimulus
204421_s_at	FGF2	Activation of MAPKK activity, activation of MAPK activity, MAPK import into nucleus, angiogenesis, branching involved in ureteric bud morphogenesis, organ induction, positive regulation of protein phosphorylation, positive regulation of endothelial cell proliferation, cell migration involved in sprouting angiogenesis, regulation of transcription, DNA-dependent, phosphatidylinositol biosynthetic process, C21-steroid hormone biosynthetic process, apoptotic process, chemotaxis, signal transduction, epidermal growth factor receptor signaling pathway, intracellular protein kinase cascade, Ras protein signal transduction, synaptic transmission, multicellular organismal development, nervous system development, positive regulation of cell proliferation, negative regulation of cell proliferation, insulin receptor signaling pathway, fibroblast growth factor receptor signaling pathway, fibroblast growth factor receptor signaling pathway, embryo development, organ morphogenesis, glial cell differentiation, positive regulation of endothelial cell migration, positive regulation of gene expression, negative regulation of fibroblast migration, positive regulation of phospholipase C activity, regulation of calcium ion-dependent exocytosis, substantia nigra development, positive regulation of cerebellar granule cell precursor proliferation, cell differentiation, extracellular matrix organization, hyaluronan catabolic process, negative regulation of cell growth, lung development, inositol phosphate biosynthetic process, Fc-epsilon receptor signaling pathway, wound healing, positive regulation of cell fate specification, positive regulation of blood vessel endothelial cell migration, negative regulation of blood vessel endothelial cell migration, positive regulation of phosphatidylinositol 3-kinase activity, innate immune response, positive regulation of cell differentiation, positive regulation of osteoblast differentiation, regulation of angiogenesis, positive regulation of angiogenesis, negative regulation of transcription, DNA-dependent, positive regulation of transcription, DNA-dependent, positive regulation of transcription from RNA polymerase II promoter, regulation of retinal cell programmed cell death, neurotrophin TRK receptor signaling pathway, phosphatidylinositol-mediated signaling, embryonic morphogenesis, response to axon injury, stem cell development, positive regulation of epithelial cell proliferation, positive chemotaxis, release of sequestered calcium ion into cytosol, regulation of cell cycle, positive regulation of cell division, positive regulation of cardiac muscle cell proliferation, corticotropin hormone secreting cell differentiation, thyroid-stimulating hormone-secreting cell differentiation, negative regulation of cell death, chondroblast differentiation, mammary gland epithelial cell differentiation, negative regulation of wound healing, positive regulation of ERK1 and ERK2 cascade

Table II. Continued.

Probe set ID	Gene symbol	Gene ontology biological process
223618_at 1555471_a_at	FMN2	Transport, apoptotic process, response to stress, response to DNA damage stimulus, meiotic metaphase I, multicellular organismal development, protein transport, cellular component organization, vesicle-mediated transport, meiotic chromosome movement towards spindle pole, actin cytoskeleton organization, intracellular signal transduction, polar body extrusion after meiotic divisions, negative regulation of protein catabolic process, negative regulation of apoptotic process, actin nucleation, intracellular transport, oogenesis, establishment of meiotic spindle localization, homologous chromosome movement towards spindle pole involved in homologous chromosome segregation, formin-nucleated actin cable assembly, cellular response to hypoxia
214701_s_at 214702_at	FN1	Angiogenesis, platelet degranulation, acute-phase response, cell-substrate junction assembly, cell adhesion, cell-matrix adhesion, calcium-independent cell-matrix adhesion, blood coagulation, regulation of cell shape, response to wounding, positive regulation of peptidase activity, cell migration, peptide cross-linking, platelet activation, extracellular matrix organization, substrate adhesion-dependent cell spreading, wound healing, leukocyte migration
206307_s_at	FOXD1	Neural crest cell migration, transcription, DNA-dependent, regulation of transcription, DNA-dependent, pattern specification process, peripheral nervous system development, embryo development, positive regulation of gene expression, melanocyte differentiation, positive regulation of BMP signaling pathway, negative regulation of transcription, DNA-dependent, positive regulation of transcription from RNA polymerase II promoter, enteric nervous system development, sympathetic nervous system development, axon extension involved in axon guidance, lateral line nerve glial cell development, iridophore differentiation, regulation of sequence-specific DNA binding transcription factor activity, cartilage development, dichotomous subdivision of terminal units involved in ureteric bud branching, metanephric capsule development, metanephric capsule specification, positive regulation of kidney development
204948_s_at 207345_at 226847_at	FST	Negative regulation of transcription from RNA polymerase II promoter, hematopoietic progenitor cell differentiation, gamete generation, pattern specification process, female gonad development, BMP signaling pathway, hair follicle morphogenesis, negative regulation of activin receptor signaling pathway, odontogenesis of dentin-containing tooth, keratinocyte proliferation, negative regulation of cell differentiation, negative regulation of follicle-stimulating hormone secretion, positive regulation of hair follicle development
209905_at	HOXA10-HOXA9, HOXA9, MIR196B	Transcription, DNA-dependent, regulation of transcription, DNA-dependent, multicellular organismal development, anterior/posterior pattern specification, proximal/distal pattern formation, mammary gland development, embryonic forelimb morphogenesis, endothelial cell activation, negative regulation of myeloid cell differentiation, embryonic skeletal system development, definitive hemopoiesis
203851_at	IGFBP6	Regulation of cell growth, signal transduction, negative regulation of cell proliferation, cellular protein metabolic process
210261_at	KCNK2	Transport, ion transport, potassium ion transport, G-protein coupled receptor signaling pathway, synaptic transmission, regulation of ion transmembrane transport, potassium ion transmembrane transport
244623_at	KCNQ5	Protein complex assembly, transport, ion transport, potassium ion transport, synaptic transmission, regulation of ion transmembrane transport, transmembrane transport, potassium ion transmembrane transport
233533_at	KRTAP1-5	-
243813_at	LINC00968	-
204298_s_at 213640_s_at 215446_s_at	LOX	Blood vessel development, cellular protein modification process, response to hormone stimulus, extracellular matrix organization, collagen fibril organization, lung development, wound healing, response to drug, elastic fiber assembly, response to steroid hormone stimulus, oxidation-reduction process

Table II. Continued.

Probe set ID	Gene symbol	Gene ontology biological process
230112_at	MARCH4	Protein ubiquitination
219054_at 219789_at 219790_s_at	NPR3	Skeletal system development, osteoclast proliferation, adenylate cyclase-inhibiting G-protein coupled receptor signaling pathway, negative regulation of adenylate cyclase activity, phospholipase C-activating G-protein coupled receptor signaling pathway, regulation of blood pressure, regulation of osteoblast proliferation, positive regulation of urine volume, positive regulation of nitric-oxide synthase activity
213791_at	PENK	Behavioral fear response, signal transduction, neuropeptide signaling pathway, behavior, sensory perception of pain
207558_s_at	PITX2	Negative regulation of transcription from RNA polymerase II promoter, patterning of blood vessels, vasculogenesis, in utero embryonic development, neuron migration, extraocular skeletal muscle development, atrioventricular valve development, cardiac neural crest cell migration involved in outflow tract morphogenesis, pulmonary myocardium development, regulation of transcription, DNA-dependent, regulation of transcription from RNA polymerase II promoter, transcription from RNA polymerase II promoter, multicellular organismal development, determination of left/right symmetry, brain development, heart development, skeletal muscle tissue development, myoblast fusion, male gonad development, female gonad development, anatomical structure morphogenesis, response to hormone stimulus, organ morphogenesis, Wnt receptor signaling pathway, subthalamic nucleus development, hypothalamus cell migration, pituitary gland development, neuron differentiation, lung development, regulation of cell migration, embryonic camera-type eye development, response to vitamin A, embryonic hindlimb morphogenesis, hair cell differentiation, vascular smooth muscle cell differentiation, deltoid tuberosity development, regulation of cell proliferation, odontogenesis of dentin-containing tooth, odontogenesis, camera-type eye development, positive regulation of DNA binding, positive regulation of transcription, DNA-dependent, positive regulation of transcription from RNA polymerase II promoter, spleen development, embryonic digestive tract morphogenesis, cardiac muscle tissue development, cardiac muscle cell differentiation, atrial cardiac muscle tissue morphogenesis, ventricular cardiac muscle cell development, digestive system development, somatotropin secreting cell differentiation, prolactin secreting cell differentiation, ventricular septum morphogenesis, left lung morphogenesis, pulmonary vein morphogenesis, superior vena cava morphogenesis, endodermal digestive tract morphogenesis, iris morphogenesis, cell proliferation involved in outflow tract morphogenesis, left/right axis specification, positive regulation of myoblast proliferation
219729_at	PRRX2	Positive regulation of mesenchymal cell proliferation, regulation of transcription, DNA-dependent, multicellular organismal development, embryonic limb morphogenesis, inner ear morphogenesis, middle ear morphogenesis, positive regulation of smoothened signaling pathway, embryonic cranial skeleton morphogenesis, embryonic skeletal system morphogenesis, artery morphogenesis, cartilage development
210367_s_at	PTGES	Prostaglandin biosynthetic process, acute inflammatory response, chronic inflammatory response, lipid metabolic process, fatty acid metabolic process, fatty acid biosynthetic process, prostaglandin metabolic process, signal transduction, negative regulation of cell proliferation, response to organic cyclic compound, arachidonic acid metabolic process, cyclooxygenase pathway, response to lipopolysaccharide, response to retinoic acid, response to cytokine stimulus, small molecule metabolic process, response to calcium ion
206157_at	PTX3	Response to yeast, inflammatory response, opsonization, positive regulation of nitric oxide biosynthetic process, positive regulation of phagocytosis
239202_at	RAB3B	GTP catabolic process, transport, intracellular protein transport, nucleocytoplasmic transport, signal transduction, small GTPase mediated signal transduction, protein transport, regulation of exocytosis, peptidyl-cysteine methylation
235417_at	SPOCD1	Transcription, DNA-dependent, negative regulation of phosphatase activity
203438_at	STC2	Cellular calcium ion homeostasis, response to oxidative stress, cell surface receptor signaling

Table II. Continued.

Probe set ID	Gene symbol	Gene ontology biological process
203439_s_at		pathway, cell-cell signaling, embryo implantation, response to nutrient, endoplasmic reticulum unfolded protein response, response to vitamin D, response to endoplasmic reticulum stress, negative regulation of multicellular organism growth, response to peptide hormone stimulus, decidualization, calcium ion homeostasis, cellular response to hypoxia, regulation of store-operated calcium entry
201107_s_at	THBS1	Activation of MAPK activity, response to hypoxia, negative regulation of endothelial cell proliferation, negative regulation of cell-matrix adhesion, sprouting angiogenesis, chronic inflammatory response, platelet degranulation, negative regulation of antigen processing and presentation of peptide or polysaccharide antigen via MHC class II, negative regulation of dendritic cell antigen processing and presentation, outflow tract morphogenesis, endocardial cushion development, growth plate cartilage development, induction of apoptosis, inflammatory response, immune response, cell cycle arrest, cell adhesion, blood coagulation, response to glucose stimulus, positive regulation of endothelial cell migration, negative regulation of endothelial cell migration, negative regulation of plasma membrane long-chain fatty acid transport, negative regulation of nitric oxide mediated signal transduction, negative regulation of cGMP-mediated signaling, negative regulation of plasminogen activation, positive regulation of macrophage chemotaxis, positive regulation of fibroblast migration, positive regulation of cell-substrate adhesion, cell migration, negative regulation of angiogenesis, peptide cross-linking, platelet activation, positive regulation of blood coagulation, extracellular matrix organization, positive regulation of cell migration, positive regulation of transforming growth factor beta receptor signaling pathway, response to magnesium ion, response to progesterone stimulus, negative regulation of interleukin-12 production, positive regulation of transforming growth factor beta1 production, cellular response to heat, response to endoplasmic reticulum stress, negative regulation of fibroblast growth factor receptor signaling pathway, positive regulation of phosphorylation, response to drug, positive regulation of tumor necrosis factor biosynthetic process, positive regulation of macrophage activation, negative regulation of apoptotic process, negative regulation of cysteine-type endopeptidase activity involved in apoptotic process, positive regulation of blood vessel endothelial cell migration, negative regulation of blood vessel endothelial cell migration, engulfment of apoptotic cell, positive regulation of translation, positive regulation of angiogenesis, behavioral response to pain, blood vessel morphogenesis, positive regulation of chemotaxis, response to calcium ion, negative regulation of focal adhesion assembly, positive regulation of protein kinase B signaling cascade, negative regulation of fibrinolysis, positive regulation of execution phase of apoptosis, positive regulation of extrinsic apoptotic signaling pathway via death domain receptors, positive regulation of endothelial cell apoptotic process, positive regulation of reactive oxygen species metabolic process, negative regulation of extrinsic apoptotic signaling pathway
201387_s_at	UCHL1	Proteolysis, ubiquitin-dependent protein catabolic process, response to stress, axonogenesis, axon target recognition, adult walking behavior, cell death, cell proliferation, protein deubiquitination, sensory perception of pain, axon transport of mitochondrion, eating behavior, negative regulation of MAP kinase activity, muscle fiber development, neuromuscular process
209946_at	VEGFC	Angiogenesis, positive regulation of neuroblast proliferation, platelet degranulation, substrate-dependent cell migration, signal transduction, multicellular organismal development, blood coagulation, positive regulation of cell proliferation, organ morphogenesis, morphogenesis of embryonic epithelium, cell differentiation, platelet activation, regulation of vascular endothelial growth factor receptor signaling pathway, positive regulation of protein autophosphorylation, response to drug, positive regulation of blood vessel endothelial cell migration, negative regulation of blood pressure, vascular endothelial growth factor receptor signaling pathway, positive regulation of epithelial cell proliferation, positive regulation of protein secretion, positive chemotaxis, induction of positive chemotaxis, positive regulation of cell division, positive regulation of mast cell chemotaxis, positive regulation of lymphangiogenesis
232122_s_at	VEPH1	-

Table III. Common genes among the upregulated probe sets in MSCs compared with diffuse-type GC (U133Plus2.0) and the upregulated probe sets in diffuse-type GC compared with intestinal-type GC (U95Av2).

Gene symbol	U95Av2 probe set ID	U133Plus2.0 probe set ID	Ratio of MSCs (12) to GC (5)	Entrez gene ID
PENK	38291_at	213791_at	24.4	5179
VEGFC	159_at	209946_at	18.2	7424
KCNK2	34087_at	210261_at	14.7	3776
IGFBP6	1736_at	203851_at	13.3	3489
RGS4	34272_at	204338_s_at	13.2	5999
MFAP5	36513_at	209758_s_at	11.5	8076
COMP	40162_s_at	205713_s_at	10.5	1311
ITGBL1	40681_at	231993_at	9.5	9358
MAP1B	39531_at	214577_at	9.4	4131
SERPINE2	41246_at	212190_at	8.1	5270
CRYAB	32243_g_at	209283_at	8.1	1410
TPM2	32314_g_at	212654_at	8.0	7169
NOV	39250_at	214321_at	8.0	4856
CYP1B1	859_at	202435_s_at	7.4	1545
TUSC3	36851_g_at	209228_x_at	7.3	7991
LTBP2	37906_at	204682_at	7.3	4053
LEPR	34267_r_at	211354_s_at	7.2	3953
FBN1	32535_at	202765_s_at	6.8	2200
PPP1R3C	39366_at	204284_at	6.6	5507
LOXL1	36811_at	203570_at	6.3	4016
PRKD1	123_at	205880_at	6.0	5587
CXCL12	33834_at	203666_at	5.5	6387
GAS6	1597_at	202177_at	5.4	2621
NUPR1	38754_at	209230_s_at	5.4	26471
NNMT	37032_at	202238_s_at	5.3	4837
CALD1	41739_s_at	201615_x_at	5.3	800
ARMCX2	36057_at	203404_at	5.0	9823
SGCB	37223_at	205120_s_at	5.0	6443
FGF7	1380_at	205782_at	5.0	2252
MXRA7	41273_at	235836_at	4.9	439921
AXL	1278_at	202686_s_at	4.9	558
CDH11	2087_s_at	207172_s_at	4.9	1009
ACTC1	39063_at	205132_at	4.8	70
NAV3	33235_at	204823_at	4.7	89795
THBS2	658_at	203083_at	4.5	7058
ELN	39098_at	212670_at	3.8	2006
STAC	40024_at	205743_at	3.8	6769
TPM1	36792_at	206117_at	3.8	7168
RECK	35234_at	205407_at	3.6	8434
DDR2	1319_at	227561_at	3.5	4921
DOK5	40401_at	214844_s_at	3.4	55816
PRUNE2	33442_at	212806_at	3.4	158471
GLRB	39665_at	205280_at	3.3	2743
DZIP1	36521_at	204556_s_at	3.3	22873
SGCD	41378_at	214492_at	3.3	6444
PCOLCE	31609_s_at	202465_at	3.3	5118
COX7A1	39031_at	204570_at	3.2	1346
EFEMP1	32551_at	201843_s_at	3.2	2202
PTRF	34320_at	208789_at	3.2	284119

Table III. Continued.

Gene symbol	U95Av2 probe set ID	U133Plus2.0 probe set ID	Ratio of MSCs (12) to GC (5)	Entrez gene ID
ACTN1	39330_s_at	211160_x_at	3.1	87
PTGIS	36533_at	208131_s_at	3.0	5740
FEZ1	37743_at	203562_at	3.0	9638
EYA2	35226_at	209692_at	3.0	2139
CAP2	693_g_at	212554_at	3.0	10486
FERMT2	36577_at	214212_x_at	3.0	10979
TMEM47	37958_at	209655_s_at	2.9	83604
FAM127A	33856_at	201828_x_at	2.9	8933
RHOBTB3	32216_r_at	202976_s_at	2.8	22836
FAP	39945_at	209955_s_at	2.8	2191
LTBP1	1495_at	202728_s_at	2.7	4052
COL8A1	37459_at	226237_at	2.7	1295
BICC1	39506_at	213429_at	2.6	80114
CAV1	36119_at	203065_s_at	2.6	857
NAP1L3	743_at	204749_at	2.6	4675
CLIP3	36095_at	212358_at	2.5	25999
ZNF423	34950_at	214761_at	2.5	23090
GAS1	661_at	204457_s_at	2.5	2619
OBSL1	35781_g_at	212776_s_at	2.3	23363
IGFBP4	1737_s_at	201508_at	2.3	3487
COL6A2	34802_at	213290_at	2.2	1292
NR3C1	706_at	216321_s_at	2.2	2908
THY1	39395_at	208850_s_at	2.2	7070
KCNMA1	40737_at	221584_s_at	2.1	3778
SLC16A4	39260_at	205234_at	2.1	9122
SORBS2	39295_s_at	204288_s_at	2.1	8470
CDK5	1206_at	204247_s_at	2.1	1020
PALLD	41191_at	200906_s_at	2.0	23022

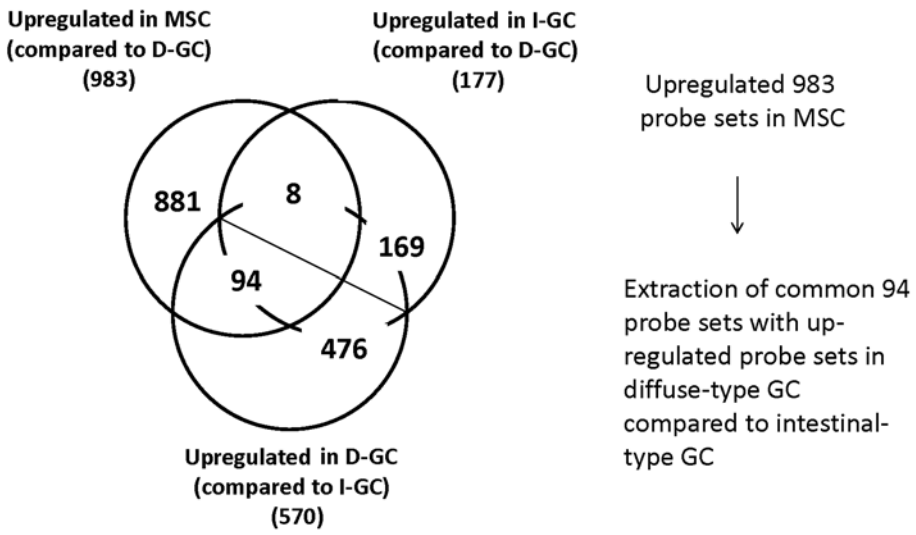

Figure 2. Venn diagram of the extraction of common genes with upregulated probe sets in MSCs and upregulated probe sets in diffuse-type GC. Probe sets with an average signal intensity of >500 in MSCs and greater than a 2-fold change in MSCs compared with diffuse-type GC were selected from the U133Plus2.0 platform and were aligned with the U95Av2 platform. Furthermore, 94 probe sets were extracted that were upregulated in diffuse-type GC compared with intestinal-type GC on the U95Av2 platform.

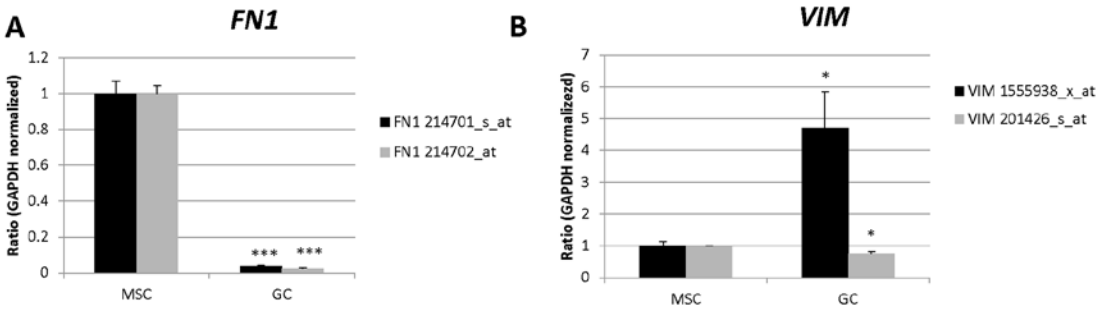

Figure 3. Gene expression of *FN1* (A) and *VIM* (B). (A) *FN1* gene expression was upregulated in MSCs compared with diffuse-type GC. (B) One of the probe sets recognizing *VIM* was downregulated in MSCs compared with diffuse-type GC. The data are presented as the mean ± SE of the ratio to the average in the MSCs (***P<0.001 and *P<0.05 vs. MSCs; n=12 MSCs and n=5 diffuse-type GC). The data were normalized to *GAPDH*.

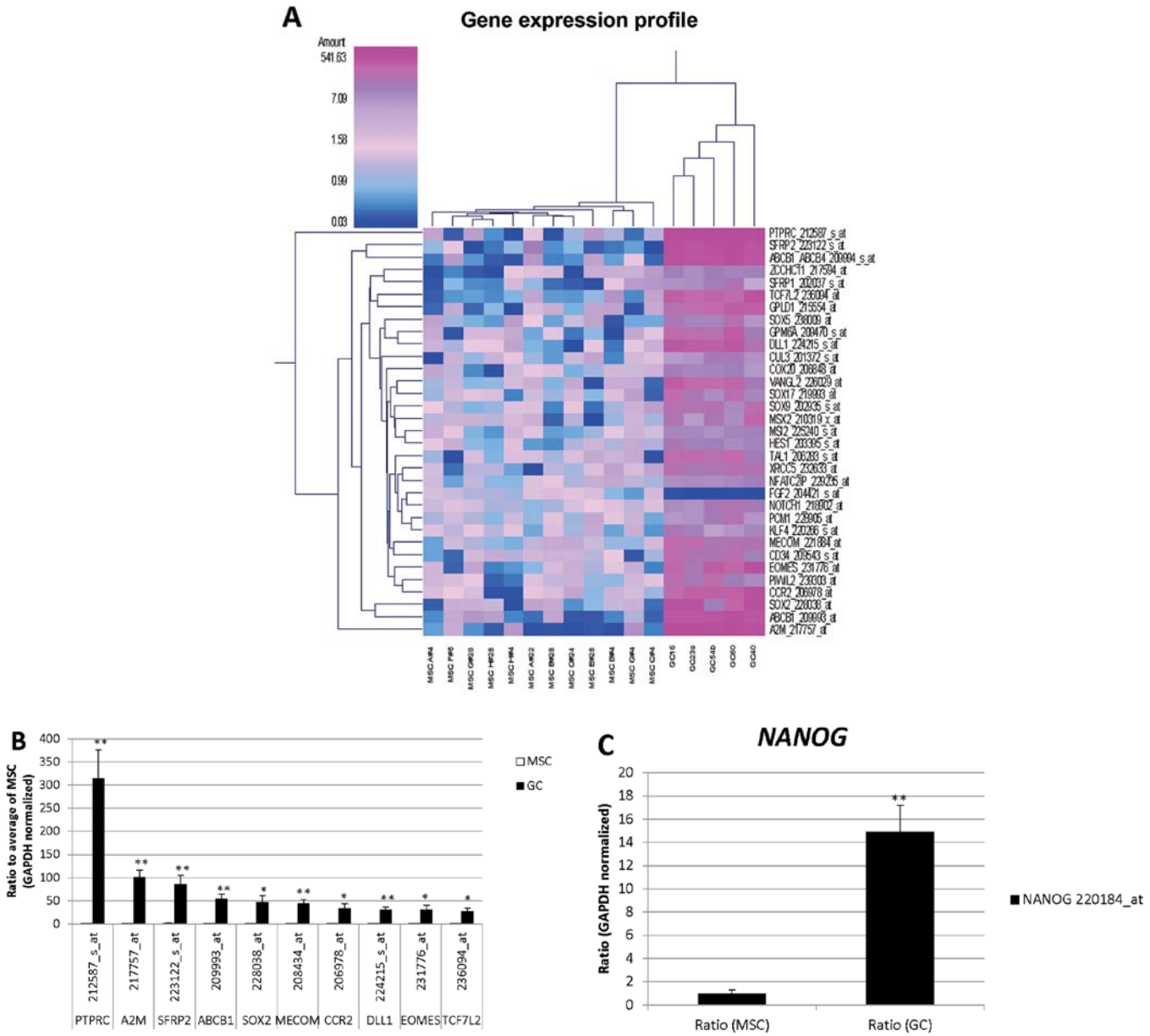

Figure 4. Gene expression of stem cell-related genes in MSCs and diffuse-type GC. (A) The gene expression of 33 stem cell-related genes, which were selected based on biological processes using gene ontology, in MSCs and diffuse-type GC was compared by clustering analysis (fold change >5 in diffuse-type GC compared with MSCs) (NCSS 2007). The amount value is indicated as the ratio to the average *GAPDH*-normalized signal intensity in the MSCs. (B) From among the 33 stem cell-related genes, 10 probe sets with a >20-fold change in diffuse-type GC compared with MSCs are shown. The data are presented as the mean ± SE of the ratio to the average in the MSCs (**P<0.01, *P<0.05 vs. MSCs; n=12 MSCs and n=5 diffuse-type GC). The data were normalized to *GAPDH*. (C) *NANOG* gene expression was upregulated in diffuse-type GC compared with MSCs. The data are presented as the mean ± SE of the ratio to the average in the MSCs (**P<0.01 vs. MSCs; n=12 MSCs and n=5 diffuse-type GC). The data were normalized to *GAPDH*.

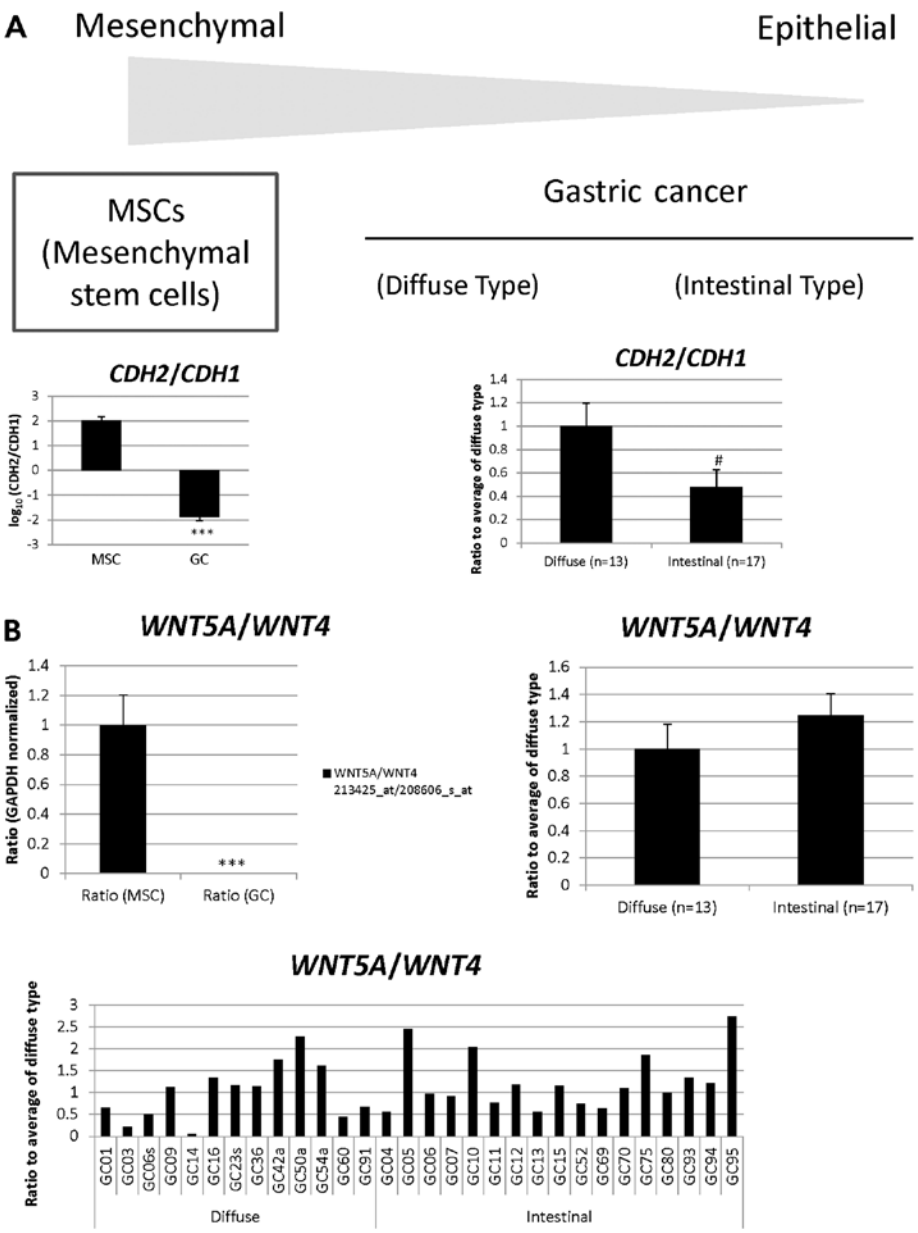

Figure 5. Diagram of the cellular phenotype transition and the mRNA ratios of *CDH2* to *CDH1* and *WNT5A* to *WNT4* in MSCs and GC. (A) A diagram of the mesenchymal to epithelial transition in MSCs, diffuse-type GC, and intestinal-type GC is shown (upper). The mRNA ratio of *CDH2* to *CDH1* in MSCs, diffuse-type GC, and intestinal-type GC was compared. (B) The mRNA ratio of *WNT5A* and *WNT4* was also examined. The data are presented as the mean ± SE of the ratio to the average in the MSCs (***P<0.001 vs. MSCs; n=12 MSCs and n=5 diffuse-type GC) or the ratio to the average in diffuse-type GC (#P<0.05 vs. diffuse-type GC; n=13 diffuse-type GC and n=17 intestinal-type GC).

manner in certain types of cancer (20-22). *NOTCH1*, which plays a well-known role in cancer development and EMT, was also upregulated in diffuse-type GC compared with MSCs. *ID3* was downregulated in diffuse-type GC compared with MSCs. *NANOG* (*Nanog homeobox*), which is involved in maintaining the pluripotency of embryonic stem cells, was upregulated in diffuse-type GC compared with MSCs (Fig. 4C). NANOG functions in conjunction with ten-eleven translocation (TET) family proteins, and TET1 enhances the efficacy of reprogramming (23). *TET1* was also upregulated in diffuse-type GC compared with MSCs.

These data indicating that embryonic stem cell-related genes may play a role in cancer cells in which EMT occurs, such as in diffuse-type GC rather than in MSCs, are very interesting; however, if particular EMT markers are overexpressed in MSCs, then these genes are unlikely to be useful for distinguishing diffuse-type GC from intestinal-type GC.

The mRNA ratio of CDH2 to CDH1 distinguished the mesenchymal from the epithelial phenotype. Using the microarray results, the mRNA ratios of *CDH2* to *CDH1* were compared in 12 MSC samples and 5 diffuse-type GC samples, and in 13 diffuse-type GC samples and 17 intestinal-type GC samples. The results and a diagram showing the phenotypic transition among the samples are shown in Fig. 5A. The mRNA ratio of *CDH2*/*CDH1* was higher in MSCs than in diffuse-type GC. The mRNA ratio of *CDH2*/*CDH1* was also higher in diffuse-type GC samples than in intestinal-type GC

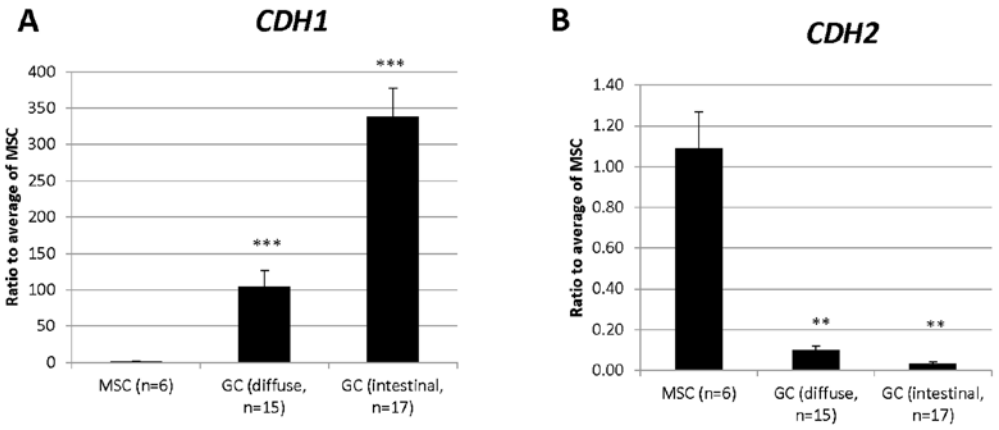

Figure 6. Quantitative real-time RT-PCR analysis of two cadherin genes. (A) *CDH1* was upregulated in the 15 diffuse-type and the 17 intestinal-type GC samples compared with the 6 MSC samples. *CDH1* mRNA expression was significantly higher in the 17 intestinal-type GC samples than in the 15 diffuse-type GC samples. (B) *CDH2* was downregulated in both GC types compared with the 6 MSC samples. *CDH2* mRNA expression was significantly lower in the 17 intestinal-type GC samples than in the 15 diffuse-type GC samples. The data are presented as the mean ± SE of the ratio to the average in the MSCs (***P<0.001, **P<0.01 vs. MSCs; n=6 MSCs, n=15 diffuse-type GC and n=17 intestinal-type GC). The data were normalized to *ACTB*.

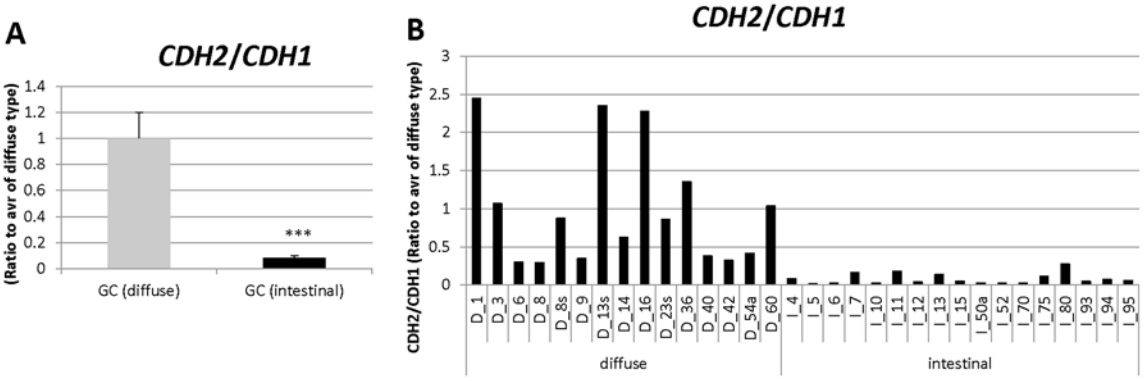

Figure 7. The *CDH2* to *CDH1* mRNA ratio obtained by quantitative real-time RT-PCR in diffuse-type GC and intestinal-type GC. (A) The *CDH2* to *CDH1* mRNA ratio was significantly higher in diffuse-type GC than in intestinal-type GC. (B) The ratios in the two types of GC were compared. The data are presented as the mean ± SE of the ratio to the average in the diffuse-type GC samples (***P<0.001 vs. diffuse-type GC; n=15 diffuse-type GC and n=17 intestinal-type GC).

samples. The combination of the *CDH2* and *CDH1* mRNA levels may distinguish the mesenchymal cell phenotype from the epithelial cell phenotype. WNT5A upregulation has been reported to be associated with EMT (7). The *WNT5A*/*WNT4* ratio was higher in MSCs than in diffuse-type GC, whereas the *WNT5A*/*WNT4* ratio was similar in the diffuse- and intestinal-type GCs (Fig. 5B). Accordingly, the combination of *WNT5A* and *WNT4* may only distinguish MSCs from GC.

We performed quantitative real-time RT-PCR to detect the expression of *CDH1* and *CDH2* in 6 MSC samples, 15 diffuse-type GC samples and 17 intestinal-type GC samples. In accordance with the above microarray results, *CDH1* was upregulated and *CDH2* was downregulated in GC compared with MSCs (Fig. 6). The *CDH2*/*CDH1* mRNA ratio was confirmed to be higher in MSCs than in both types of GC. Most importantly, the *CDH2*/*CDH1* mRNA ratio was perfect at distinguishing the 15 diffuse-type GC samples from the 17 intestinal-type GC samples (Fig. 7); all of the 15 diffuse-type GC samples had ratios that were higher than the intestinal-type GC sample with the highest ratio (I-80).

VIM is one of the most validated EMT markers. Therefore, using quantitative real-time RT-PCR, we investigated the possibility that the combination of *VIM* and *CDH1* could distinguish the mesenchymal phenotype from the epithelial phenotype (Fig. 8). The *VIM*/*CDH1* mRNA ratio was higher in MSCs than in both types of GC. However, the *VIM*/*CDH1* ratio was much more varied among the 32 GC samples than the *CDH2*/*CDH1* ratio. As mentioned above, there was a threshold *CDH2*/*CDH1* ratio that distinguished the 15 diffuse-type GC samples from the 17 intestinal-type GC samples, whereas some intestinal-type GC samples (for example, I-11 and I-15) had a higher *VIM*/*CDH1* ratio than certain diffuse-type GC samples.

Discussion

We previously compared the expression profiles of 18 intestinal-type GC and 12 diffuse-type GC samples with typical characteristics in terms of cell growth (clustered or scattered) and differentiation (well/moderate or poor), and selected genes based on their expression levels in the two types of cancer (7).

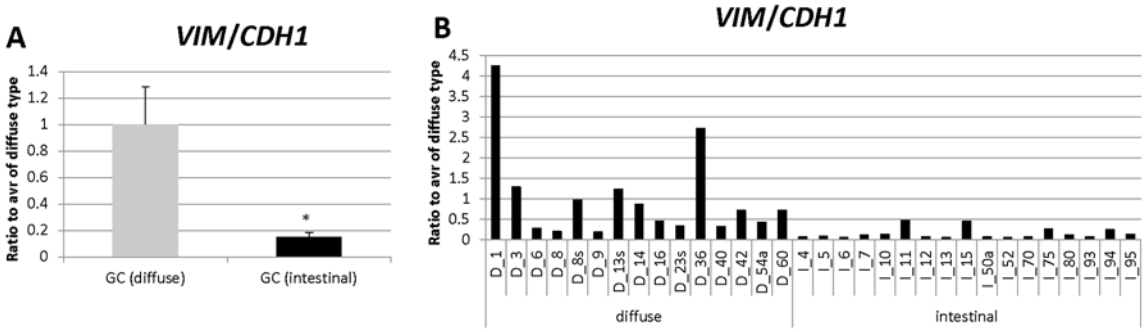

Figure 8. The *VIM* to *CDH1* mRNA ratio obtained by quantitative real-time RT-PCR in diffuse-type GC and intestinal-type GC. (A) The *VIM* to *CDH1* mRNA ratio was significantly higher in diffuse-type GC than in intestinal-type GC. (B) The ratios in the two types of GC were compared. The data are presented as the mean ± SE of the ratio to the average in the diffuse-type GC samples (*P<0.05 vs. diffuse-type GC; n=15 diffuse-type GC and n=17 intestinal-type GC).

A gene was selected using the Wilcoxon U test (P<0.05) from genes with more than a 2-fold change on average. By this procedure, a total of 892 genes were identified (704 genes specific to diffuse-type and 188 genes specific to intestinal-type). The two types of GC were completely separated by two-dimensional hierarchical clustering analysis of the 892 selected genes. In this paper, we reported that an EMT regulator, *ZEB1*/*SIP1*, is a target of the primary transcription factor GLI1 in the Hh signaling pathway in diffuse-type GC and that *ZEB1*/*SIP1* further activates *NOTCH2* and other EMT regulators [snail family zinc finger 2 (*SNAI2*) and twist family bHLH transcription factor 2 (*TWIST2*)]. *SNAI2* upregulates *CDH2* and *WNT5A* and downregulates *CDH1*. *TWIST2* upregulates *CDH2*, *ROR2*, which is the WNT5A receptor, and other mesenchymal-related genes (*PDGFRB*, *EDNRA*, *ROBO1* and *MEF2C*). Accordingly, we concluded that Hh signaling-mediated EMT specifically occurred in diffuse-type GC. This crosstalk between Hh signaling and EMT has been reported in esophageal squamous cell carcinoma (24). However, we were unable to identify a single marker that distinguished the 12 diffuse-type GC samples from the 18 intestinal-type GC samples. Therefore, herein, we searched for such genes by comparing the expression profiles of diffuse-type GC and MSCs, which are typical mesenchymal cells. Among the 1461 probe sets that were significantly upregulated in MSCs, we selected 94 probes (77 genes) that were upregulated in diffuse-type GC compared with intestinal-type GC (Table III).

The typical mesenchymal cell markers *FN1*, *VIM* and *CDH2* were highly expressed in MSCs. Regarding EMT regulators, it is known that the Snail family transcription factor regulates EMT by repressing *CDH1* gene transcription (25). *SNAI2* expression was higher in MSCs than in diffuse-type GC. *CDH1* gene regulation might be involved in EMT because it was shown that intracellular CDH1 is located at the membrane after treatment with siRNA targeting the EMT regulator *ZEB2*/*SIP1* in esophageal cancer (24). In terms of Wnt signaling, *WNT5A* was upregulated in MSCs compared with diffuse-type GC; however, its receptor *ROR2* was more highly expressed in diffuse-type GC than in MSCs. Regarding Notch signaling, *NOTCH1*, *3* and *4* were highly expressed in the diffuse-type GC samples, whereas *NOTCH2* was upregulated in MSCs. Because NOTCH is related to stem cell maintenance, this alteration in gene expression may reflect transitions or modifications in stem cell features (26). In terms of other stem cell markers, a recent report suggested that $Lgr5^+$ cells in mouse intestinal adenomas acquired the ability for cancerous growth as a stem cell (27). Dclk1 (doublecortin-like kinase 1), which is a candidate marker for intestinal cancer stem cells, did not dramatically differ in expression between diffuse-type GC and MSCs (28).

From these results, we selected *FN1*, *VIM*, *CDH2*, *SNAI2*, *WNT5A* and *NOTCH2* as EMT-related genes that were upregulated in MSCs. However, all 6 of these genes were included in our previously-selected 704 genes that were upregulated in diffuse-type GC compared with intestinal-type GC. Therefore, we examined the power of the mRNA ratio of each of these 6 mesenchymal-related genes to a typical epithelial marker gene, *CDH1*. We determined that the mRNA ratio of *CDH2* to *CDH1* has great potential as a single indicator that distinguishes diffuse-type GC from intestinal-type GC. In the near future, the power of this simple indicator of EMT should be evaluated in a large cohort study of GC as well as other tumor types.

Acknowledgements

We gratefully acknowledge Dr Ryoji Kushima for the pathological and clinical evaluations. We would also like to thank Ms. Rie Komatsuzaki and Ms. Fumiko Chiwaki for their technical assistance. This study was supported in part by the National Institute of Biomedical Innovation (for the Advanced Research for Medical Products Mining Programme ID10-41, ID12-01), the Ministry of Health, Labour and Welfare of Japan (for the Third Comprehensive 10-Year Strategy for Cancer Control H22-007 and for Cancer Control and Cancer Research 20-12), National Cancer Center Research and Development Fund (23-A-7, 23-B-6, 23-B-18, 25-A-6), the Ministry of Education, Culture, Sports, Science and Technology of Japan (23501322) and the Princess Takamatsu Cancer Research Fund.

References

1. Radisky DC and LaBarge MA: Epithelial-mesenchymal transition and the stem cell phenotype. Cell Stem Cell 2: 511-512, 2008.
2. Mani SA, Guo W, Liao MJ, *et al*: The epithelial-mesenchymal transition generates cells with properties of stem cells. Cell 133: 704-715, 2008.

3. Vogelstein B, Papadopoulos N, Velculescu VE, *et al*: Cancer genome landscapes. Science 339: 1546-1558, 2013.
4. Saeki N, Saito A, Choi IJ, *et al*: A functional single nucleotide polymorphism in mucin 1, at chromosome 1q22, determines susceptibility to diffuse-type gastric cancer. Gastroenterology 140: 892-902, 2011.
5. Sakamoto H, Yoshimura K, Saeki N, *et al*: Genetic variation in PSCA is associated with susceptibility to diffuse-type gastric cancer. Nat Genet 40: 730-740, 2008.
6. Fukaya M, Isohata N, Ohta H, *et al*: Hedgehog signal activation in gastric pit cell and in diffuse-type gastric cancer. Gastroenterology 131: 14-29, 2006.
7. Ohta H, Aoyagi K, Fukaya M, *et al*: Cross talk between hedgehog and epithelial-mesenchymal transition pathways in gastric pit cells and in diffuse-type gastric cancers. Br J Cancer 100: 389-398, 2009.
8. Ueda T, Volinia S, Okumura H, *et al*: Relation between microRNA expression and progression and prognosis of gastric cancer: a microRNA expression analysis. Lancet Oncol 11: 136-146, 2010.
9. Kountouras J, Zavos C and Chatzopoulos D: New concepts of molecular biology on gastric carcinogenesis. Hepatogastroenterology 52: 1305-1312, 2005.
10. Tanabe S, Sato Y, Suzuki T, *et al*: Gene expression profiling of human mesenchymal stem cells for identification of novel markers in early- and late-stage cell culture. J Biochem 144: 399-408, 2008.
11. Aoyagi K, Minashi K, Igaki H, *et al*: Artificially induced epithelial-mesenchymal transition in surgical subjects: its implications in clinical and basic cancer research. PLoS One 6: e18196, 2011.
12. Edgar R, Domrachev M and Lash AE: Gene Expression Omnibus: NCBI gene expression and hybridization array data repository. Nucleic Acids Res 30: 207-210, 2002.
13. Sigurdsson V, Hilmarsdottir B, Sigmundsdottir H, *et al*: Endothelial induced EMT in breast epithelial cells with stem cell properties. PLoS One 6: e23833, 2011.
14. Guillot C and Lecuit T: Mechanics of epithelial tissue homeostasis and morphogenesis. Science 340: 1185-1189, 2013.
15. Gupta PB, Onder TT, Jiang G, *et al*: Identification of selective inhibitors of cancer stem cells by high-throughput screening. Cell 138: 645-659, 2009.
16. Elenbaas B, Spirio L, Koemer F, *et al*: Human breast cancer cells generated by oncogenic transformation of primary mammary epithelial cells. Gene Dev 15: 50-65, 2001.
17. Lu D, Choi MY, Yu J, *et al*: Salinomycin inhibits Wnt signaling and selectivity induces apoptosis in chronic lymphocytic leukemia cells. Proc Natl Acad Sci USA 108: 13253-13257, 2011.
18. Huch M, Dorrell C, Boj SF, *et al*: *In vitro* expansion of single Lgr5$^+$ liver stem cells induced by Wnt-driven regeneration. Nature 494: 247-250, 2013.
19. Nishimura K, Semba S, Aoyagi K, *et al*: Mesenchymal stem cells provide an advantageous tumor microenvironment for the restoration of cancer stem cells. Pathobiology 79: 290-306, 2012.
20. Rudin CM, Durinck S, Stawiski EW, *et al*: Comprehensive genomic analysis identifies SOX2 as a frequently amplified gene in small-cell lung cancer. Nat Genet 44: 1111-1116, 2012.
21. Jia X, Li X, Xu Y, *et al*: SOX2 promotes tumorigenesis and increases the anti-apoptotic property of human prostate cancer cell. J Mol Cell Biol 3: 230-238, 2011.
22. Bass AJ, Watanabe H, Mermel CH, *et al*: SOX2 is an amplified lineage-survival oncogene in lung and esophageal squamous cell carcinomas. Nat Genet 41: 1238-1242, 2009.
23. Costa Y, Ding J, Theunissen TW, *et al*: NANOG-dependent function of TET1 and TET2 in establishment of pluripotency. Nature 495: 370-374, 2013.
24. Isohata N, Aoyagi K, Mabuchi T, *et al*: Hedgehog and epithelial-mesenchymal transition signaling in normal and malignant epithelial cells of the esophagus. Int J Cancer 125: 1212-1221, 2009.
25. Cano A, Pérez-Moreno MA, Rodrigo I, *et al*: The transcription factor snail controls epithelial-mesenchymal transitions by repressing E-cadherin expression. Nat Cell Biol 2: 76-83, 2000.
26. Sato T and Clevers H: Growing self-organizing mini-guts from a single intestinal stem cell: mechanism and applications. Science 340: 1190-1194, 2013.
27. Schepers AG, Snippert HJ, Stange DE, *et al*: Lineage tracing reveals Lgr5$^+$ stem cell activity in mouse intestinal adenomas. Science 337: 730-735, 2012.
28. Nakanishi Y, Seno H, Fukuoka A, *et al*: Dclk1 distinguishes between tumor and normal stem cells in the intestine. Nat Genet 45: 98-103, 2013.